Mono- and Di-dentate Tertiary Phosphine and Monodentate Tertiary Phosphite Derivatives of $[Ru_4H(CO)_{12}BH_2]$†

Sylvia M. Draper,[a] Catherine E. Housecroft,*[,b] James S. Humphrey[a] and Arnold L. Rheingold*[,c]

[a] *University Chemical Laboratory, Lensfield Road, Cambridge CB2 1EW, UK*

[b] *Institut für Anorganische Chemie, Spitalstrasse 51, CH-4056 Basel, Switzerland*

[c] *Department of Chemistry, University of Delaware, Newark, DE 19716, USA*

The reactions of the butterfly cluster $[Ru_4H(CO)_{12}BH_2]$ with a range of tertiary phosphines and diphosphines and with a large excess of trimethyl phosphite have been explored. Twenty-two derivatives of the general types $[Ru_4H(CO)_{12-x}(PR_3)_xBH_2]$ (x = 1 or 2), $[Ru_4H(CO)_{12-x}\{P(OMe)_3\}_xBH_2]$ (x = 2–4), $[Ru_4H(CO)_{11}(L\text{–}L)BH_2]$, $[Ru_4H(CO)_{10}(L\text{–}L)BH_2]$ and $[\{Ru_4H(CO)_{11}BH_2\}_2\{\mu\text{-}(L\text{–}L)\}]$ (L–L = diphosphine) have been synthesised and characterised by mass spectrometry and IR and multinuclear NMR spectroscopies. The single-crystal structures of $[Ru_4H(CO)_{11}(PPh_3)BH_2]$, *trans*-$[Ru_4H(CO)_{10}\{P(OMe)_3\}_2BH_2]$ and $[Ru_4H(CO)_{10}(dppe)BH_2]\cdot CH_2Cl_2$ (dppe = $Ph_2PCH_2CH_2PPh_2$) have been determined. In $[Ru_4H(CO)_{11}(PPh_3)BH_2]$ the PPh_3 ligand occupies a wing-tip equatorial site. In $[Ru_4H(CO)_{10}\{P(OMe)_3\}_2BH_2]$ the two $P(OMe)_3$ ligands are also in such sites and both the isomers in which these ligands are mutually *cis* or *trans* with respect to the cluster core are formed; the solid-state structure of the *trans* isomer has been confirmed. When the two phosphorus-donor atoms are provided in the form of a didentate ligand the sites of co-ordination depend upon the nature of the backbone of the ligand. In $[Ru_4H(CO)_{10}(dppe)BH_2]$, the dppe ligand bridges a $Ru_{wing\ tip}$–Ru_{hinge} edge and two isomers are observed in solution; the solid-state structure of one isomer has been elucidated. Use of the diphosphine ligands allows the formation of linked dicluster species, and the competition for the formation of linked and monocluster species in which the ligand behaves in either a mono- or di-dentate fashion has been investigated. In the case of dppa [bis(diphenylphosphino)acetylene] an additional product when the ligand is in a four-fold excess is $[Ru_4H(CO)_{10}(dppa)_2BH_2]$ in which both dppa ligands are pendant and co-ordinated to different wing-tip ruthenium atoms.

The butterfly cluster $[Ru_4H(CO)_{12}BH_2]$ was first prepared as a by-product in the reduction of $[Ru_3(CO)_{12}]$ by $[BH_4]^-$,[1] but its structure was not confirmed until over a decade later when Shore and co-workers[2] prepared the cluster from $[Ru_4H_4(CO)_{12}]$ and BH_3·thf (thf = tetrahydrofuran). We independently reported $[Ru_4H(CO)_{12}BH_2]$ as one product in the reaction of $[Ru_3(CO)_{12}]$ with BH_3·thf and $Li[BHEt_3]$ followed by addition of acid.[3] In the past few years we have been particularly concerned with aspects of homo- and hetero-metallic boride clusters[4,5] and $[Ru_4H(CO)_{12}BH_2]$ and its conjugate base have figured as precursors in some of this work. To date, however, relatively straightforward reactions of $[Ru_4H(CO)_{12}BH_2]$ have not been investigated; one exception has been a study of the addition of alkynes to this cluster.[6]

In this paper we report on a study which surveys the reactivity of $[Ru_4H(CO)_{12}BH_2]$ with tertiary phosphines, diphosphines and trimethyl phosphite. Previous, and related, investigations with metal butterfly clusters which contain a semiinterstitial p-block atom have included the reaction between $[Fe_4H(CO)_{12}BH]^-$ and PMe_2Ph. Both mono- and di-substituted derivatives were observed and spectroscopically characterised, and the substitution of a second CO by a phosphine ligand is accompanied by a rearrangement of the cluster-bound hydrogen atoms. It is proposed that in $[Fe_4H(CO)_{11}(PMe_2Ph)BH]^-$ and $[Fe_4(CO)_{10}(PMe_2Ph)_2BH_2]^-$, each phosphine co-ordinates to an equatorial $Fe_{wing\ tip}$ site.[7] Similarly, wing-tip substitution has been observed in $[Ru_4H(CO)_{11}\{P(OMe)_3\}N]$,[8] $[Fe_4H(CO)_{11}(PPh_3)N]$,[9] $[Fe_4(CO)_{11}(PMe_2Ph)N]^-$,[9] $[Fe_4(CO)_9(NO)(PPh_3)_2N]$,[9] $[RhRu_3H_2(\eta^5\text{-}C_5Me_5)(CO)_8(PPh_3)BH]$[10] and $[FeRu_3(CO)_{10}\{P(OMe)_3\}_2N]^-$.[11]

Of the ligands chosen for study, dppf [1,1′-bis(diphenylphosphino)ferrocene] is particularly flexible. The ferrocenyl unit of the dppf ligand has the potential to be stereochemically non-rigid with respect to mutual rotation of the two C_5H_4 rings. In the solid state free dppf has a *trans* arrangement of $Ph_2PC_5H_4$ rings,[12] as does co-ordinated dppf in linked complexes such as $[\{Mn(CO)_4Cl\}_2(\mu\text{-dppf})]$,[13] $[\{AuCl\}_2(\mu\text{-dppf})]$,[14] $[\{AuCl(dppf)\}_n]$[15] and $[(OC)_5W(\mu\text{-dppf})PtCl_2(\mu\text{-dppf})W(CO)_5]$.[16] However, in $[W_2H(CO)_8(NO)(dppf)]$,[17] in which only one end of the ligand is bound to a metal centre, the solid-state structure exhibits mutual ring positions that are twisted *ca.* 50° away from being fully staggered. Nor are they fully staggered in $[Mo(CO)_5(dppf)]$.[16] A range of examples shows that the dppf ligand can adopt a chelating mode,[12,18] illustrating that the two $Ph_2PC_5H_4$ units can be eclipsed, or may be close to being so.

Experimental

General Data.—Fourier-transform NMR spectra were recorded on a Bruker WM 250 or AM 400 spectrometer, IR spectra on a Perkin-Elmer FT 1710 spectrophotometer and FAB (fast atom bombardment) and FIB (fast ion bombardment) mass spectra on Kratos instruments with 3-nitrobenzyl alcohol as matrix.

All reactions were carried out under argon by using standard Schlenk techniques. Solvents were dried over suitable reagents and freshly distilled under N_2 before use. Separations were carried out by thin-layer plate chromatography with Kieselgel 60-PF-254 (Merck). Photolysis experiments used a mercury

† *Supplementary data available:* see Instructions for Authors, *J. Chem. Soc., Dalton Trans.*, 1995, Issue 1, pp. xxv–xxx.

high-pressure lamp with the sample contained in a quartz tube flushed with argon.

The reagents PPh_3, $P(C_6H_{11})_3$, $P(OMe)_3$, dppp $[Ph_2P(CH_2)_3PPh_2]$, dppb $[Ph_2P(CH_2)_4PPh_2]$, dpph $[Ph_2P(CH_2)_6PPh_2]$ and dppf (Aldrich) and dppa ($Ph_2PC{\equiv}CPPh_2$) and dppe $[Ph_2P(CH_2)_2PPh_2]$ (Strem) were used as received. The compound $[Ru_4H(CO)_{12}BH_2]$ was prepared as previously described,[3] and yields of new compounds (which are typical values) are with respect to $[Ru_4H(CO)_{12}BH_2]$.

Preparations.—Two general procedures were used as follows.

Method I. The compound dppa (27 mg, 0.07 mmol) was added to a solution of $[Ru_4H(CO)_{12}BH_2]$ (53 mg, 0.07 mmol) in CH_2Cl_2 (5 cm^3). The solution was stirred at room temperature for 8 d, and turned dark orange. Products were separated by TLC, eluting with CH_2Cl_2–hexane (1:1). This method (similar reaction scale and same cluster:diphosphine ratio) was also used for reactions between $[Ru_4H(CO)_{12}BH_2]$ and dppp or dppf. The reaction times and the solvents for TLC were as follows: dppp (3 d; CH_2Cl_2–hexane 2:3), dppf (8 d; CH_2Cl_2–hexane 1:3).

Method II. Triphenylphosphine (105 mg, 0.4 mmol) in CH_2Cl_2 (1 cm^3) was added to a solution of $[Ru_4H(CO)_{12}BH_2]$ (75 mg, 0.1 mmol) in CH_2Cl_2 (4 cm^3). The yellow solution was photolysed for 17 h and turned red-orange. Products were separated by TLC, eluting with CH_2Cl_2–hexane (1:3). This method (similar reaction scale and same reaction time) was also used for reactions between $[Ru_4H(CO)_{12}BH_2]$ and $P(C_6H_{11})_3$, $P(OMe)_3$, dppe, dppp, dppb, dpph, dppf or dppa. The cluster:phosphine molar ratios were typically 1:2 except in the cases of dppa (1:4) and $P(OMe)_3$ (30 fold excess; see text), and the solvent for TLC was CH_2Cl_2–hexane 1:3 except for $P(OMe)_3$ (CH_2Cl_2–hexane 2:3).

Mass spectrometric and NMR spectroscopic data for the new compounds are collected in Table 1 and IR spectroscopic data in Table 2.

Crystal Structural Determinations.—Crystallographic data for $[Ru_4H(CO)_{11}(PPh_3)BH_2]$, *trans*-$[Ru_4H(CO)_{10}\{P(OMe)_3\}_2BH_2]$ and $[Ru_4H(CO)_{10}(dppe)BH_2]\cdot CH_2Cl_2$ are collected in Table 3. All three compounds were determined photographically to possess 2/*m* Laue symmetry. The space groups were unambiguously determined from systematic absences in the diffraction data. All data sets were corrected for absorption effects. Direct methods were used to obtain the metal atom locations. For the dppe complex, a molecule of CH_2Cl_2, the recrystallisation solvent, was found accompanying the tetraruthenium cluster. All non-hydrogen atoms were anistropically refined and hydrogen atoms were idealised. All computations used versions 4 or 5 of SHELXTL software.[19] Atomic coordinates for $[Ru_4H(CO)_{11}(PPh_3)BH_2]$, *trans*-$[Ru_4H(CO)_{10}\{P(OMe)_3\}_2BH_2]$ and $[Ru_4H(CO)_{10}(dppe)BH_2]\cdot CH_2Cl_2$ are given and Tables 4, 6 and 8, respectively.

Additional material available from the Cambridge Crystallographic Data Centre comprises H-atom coordinates, thermal parameters and remaining bond lengths and angles.

Results and Discussion

Fig. 1 gives two schematic diagrams of $[Ru_4H(CO)_{12}BH_2]$ which emphasise the carbonyl orientations in this parent compound; its structure has been confirmed by X-ray crystallography[2] and the 100 MHz ^{13}C NMR spectrum (298 K) indicates that the carbonyl ligands are static on the NMR time-scale.[20] Carbonyl ligands 2, 5, 8 and 11 are described as axial, each being *trans* to a cluster-bound hydrogen atom; 1, 3, 4, 6, 7, 9, 10 and 12 are described as equatorial each being *cis* to a cluster hydrogen atom. The substitution patterns discussed below are with respect to the numbering scheme in Fig. 1.

Initial reactions between $[Ru_4H(CO)_{12}BH_2]$ and the phosphorus donors were carried out in CH_2Cl_2 at room

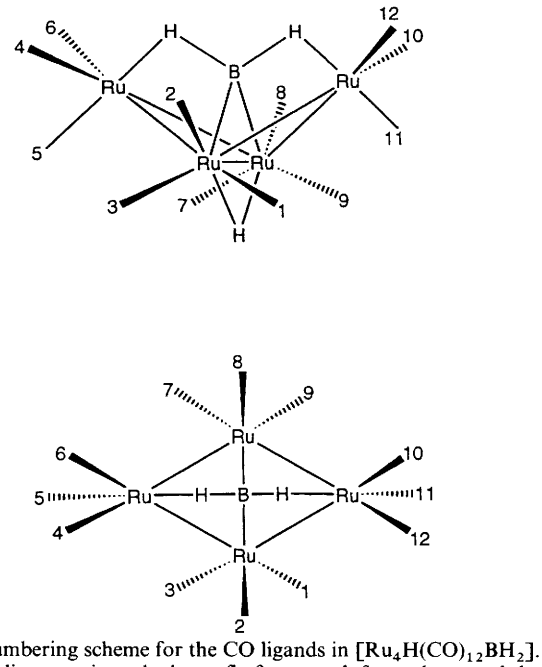

Fig. 1 Numbering scheme for the CO ligands in $[Ru_4H(CO)_{12}BH_2]$. The lower diagram views the butterfly framework from above and the hinge hydride is under the boron atom

temperature but required long time periods (typically 7–9 d); the conversion to substituted products was monitored by IR spectroscopy. Photolysis of the reaction mixture and the presence of an excess of phosphine increased the rate of reaction significantly, typical reaction times being 17–18 h.

Phosphines with One P-Donor Atom.—The reaction of $[Ru_4H(CO)_{12}BH_2]$ with a four-fold excess of PPh_3 leads to the yellow-orange compounds $[Ru_4H(CO)_{11}(PPh_3)BH_2]$ (≈45%) and $[Ru_4H(CO)_{10}(PPh_3)_2BH_2]$ (≈20%) in addition to unreacted starting material. Spectroscopic properties of these products are given in Tables 1 and 2. The ^{11}B NMR spectroscopic signals indicate that the environment around the boron atom changes little in going from $[Ru_4H(CO)_{12}BH_2]$ (^{11}B δ +109.9, $CDCl_3$) to the mono- and di-substituted derivatives. The two Ru–H–B bridging hydrogen atoms are equivalent (Fig. 1) in $[Ru_4H(CO)_{12}BH_2]$ (^1H δ −8.4, $CDCl_3$) but the ^1H NMR spectrum of $[Ru_4H(CO)_{11}(PPh_3)BH_2]$ exhibits broad signals (1:1) at δ −8.6 and −7.5. This lowering in symmetry, and the fact that the ^1H NMR spectroscopic signal assigned to the Ru–H–Ru hinge hydride is a doublet with coupling J_{PH} of only 2.0 Hz, indicates that PPh_3-for-CO substitution has occurred at a wing-tip ruthenium atom. By comparing the ^1H NMR spectral data for $[Ru_4H(CO)_{12}BH_2]$, $[Ru_4H(CO)_{11}(PPh_3)BH_2]$ and $[Ru_4H(CO)_{10}(PPh_3)_2BH_2]$ (see below), we may assign the two signals at δ −8.6 and −7.5 to the Ru–H–B protons which are, respectively, remote from and adjacent to the phosphine ligand. Substitution at an equatorial wing-tip site (*e.g.* site 4 in Fig. 1) has been confirmed by the results of an X-ray diffraction study (see below).

The high-field region of the ^1H NMR spectrum of $[Ru_4H(CO)_{10}(PPh_3)_2BH_2]$ shows that the two Ru–H–B protons are equivalent (δ −7.5) and indicates that the second PPh_3 has substituted at the second wing-tip ruthenium atom. The ^1H NMR signal for the Ru–H–Ru hydride is a triplet (J_{PH} 2.4 Hz), thus supporting the double wing-tip substitution pattern. The ^{31}P NMR spectrum exhibits two sharp resonances (δ +41.1 and +40.9) with integrals in a ratio 1:3. Referring to the numbering scheme in Fig. 1, disubstitution could occur either at sites 4 and 10 (labelled a *trans* isomer) or at 4 and 12 (labelled a *cis* isomer) and a mixture of the two isomers accounts for the observed ^{31}P NMR spectrum. It is not surprising that the ^{11}B (or the ^1H) NMR spectroscopic

Table 1 Products isolated from the reactions of $[Ru_4H(CO)_{12}BH_2]$ with PPh_3, $P(C_6H_{11})_3$, $P(OMe)_3$, dppe, dppp, dppb, dpph, dppf and dppa

Compound	Method of preparation[a]	Mass spectrometric data, *m/z* for P^+	NMR (δ, *J*/Hz)		
			$^{11}B-\{^1H\}$[b]	^{31}P[c]	^1H[d]
$[Ru_4H(CO)_{11}(PPh_3)BH_2]$	II	988 (8 CO losses)	+107.0	+41.1	+7.7–7.5 (m, Ph), −7.5 (br, Ru–H–B), −8.6 (br, Ru–H–B), −21.1 (d, J_{PH} 2.0, Ru–H–Ru)
$[Ru_4H(CO)_{10}(PPh_3)_2BH_2]$	II	1123 (10 CO losses)	+105.2	+41.1, +40.9 (2 isomers, see text)	+7.8–7.0 (m, Ph), −7.5 (br, Ru–H–B), −21.1 (t, J_{PH} 2.4, Ru–H–Ru)
$[Ru_4H(CO)_{11}\{P(C_6H_{11})_3\}BH_2]$	II	1007 (6 CO losses)	+105.9	+61.1	+2.2–1.5 (m, alkyl), −8.1 (br, Ru–H–B), −8.8 (br, Ru–H–B), −21.2 (d, J_{PH} 3.0, Ru–H–Ru)
$[Ru_4H(CO)_{10}\{P(C_6H_{11})_3\}_2BH_2]$	II	1259 (5 CO losses)	+104.9	+57.0	+2.2–1.5 (m, alkyl), −8.3 (br, Ru–H–B), −21.35 (t, J_{PH} 3.4, Ru–H–Ru)
trans-$[Ru_4H(CO)_{10}\{P(OMe)_3\}_2BH_2]$	II	946 (7 CO losses)	+105.9	+144.8	+3.9–3.5 (m, Me), −8.4 (br, Ru–H–B), −21.50 (t, J_{PH} 3.0, Ru–H–Ru)
cis-$[Ru_4H(CO)_{10}\{P(OMe)_3\}_2BH_2]$	II	946 (6 CO losses)	+108.0	+143.6	+3.8–3.5 (m, Me), −8.1 (br, Ru–H–B), −21.33 (t, J_{PH} 3.0, Ru–H–Ru)
$[Ru_4H(CO)_9\{P(OMe)_3\}_3BH_2]$	II	1042 (6 CO losses)	+107.0	+146.1 (2 P), +146.5 (1 P)	+3.7–3.3 (m, Me), −8.6 (br, Ru–H–B), −9.0 (br, Ru–H–B), −21.3 [d(J_{PH} 5) of t(J_{PH} 2), Ru–H–Ru]
$[Ru_4H(CO)_8\{P(OMe)_3\}_4BH_2]$	II	1130 (7 CO losses)	+108.6	+147.3 (2 P), +147.8 (2 P)	+3.7–3.3 (m, Me), −9.0 (br, Ru–H–B), −21.07 [t(J_{PH} 8) of t(J_{PH} 4), Ru–H–Ru]
$[Ru_4H(CO)_{10}(dppe)BH_2]$	II	1097 (10 CO losses)	+107, +112 (2 isomers, see text)	+47.9, +43.4, +40.0, +39.1 (d, J_{PH} 36) (2 isomers, see text)	+7.8–7.0 (m, Ph), +3.1 (m, CH_2), −7.6 (br, Ru–H–B), −8.1 (br, Ru–H–B), −20.60 [d(J_{PH} 5) of d(J_{PH} 1.5), Ru–H–Ru], −20.62 [d(J_{PH} 33) of d(J_{PH} 2), Ru–H–Ru]
$[\{Ru_4H(CO)_{11}BH_2\}_2$-(μ-dppe)]	II	1843 (3 CO losses)	+106.0	+34.1	+7.7–7.1 (m, Ph), +3.6 (m, CH_2), −8.3 (vbr, Ru–H–B), −21.22 (d, J_{PH} 2.3, Ru–H–Ru)
$[Ru_4H(CO)_{11}(dppp)BH_2]$	I and II	1154 (P^+ + O) (3 CO losses)	+106.4	+33.2 (1 P), −17.9 (1 P)	+7.7–7.4 (m, Ph), +3.8 (m, CH_2), +2.7 (m, CH_2), +2.5 (m, CH_2), −8.2 (br, Ru–H–B), −8.7 (br, Ru–H–B), −21.2 (d, J_{PH} 2.9, Ru–H–Ru)
$[Ru_4H(CO)_{10}(dppp)BH_2]$	II	1112 (9 CO losses)	+105.2	+32.3	+7.6–7.0 (m, Ph), +3.85 (m, CH_2), +2.75 (m, CH_2), +2.52 (m, CH_2), −7.3 (br, Ru–H–B), −8.6 (br, Ru–H–B), −21.4 (t, J_{PH} 2.3, Ru–H–Ru)
$[\{Ru_4H(CO)_{11}BH_2\}_2$(μ-dppp)]	I and II	1867 (9 CO losses)	+106.4	+31.4	+7.7–7.4 (m, Ph), +3.8 (m, CH_2), +2.7 (m, CH_2), +2.5 (m, CH_2), −8.2 (br, Ru–H–B), −8.7 (br, Ru–H–B), −21.2 (d, J_{PH} 2.9, Ru–H–Ru)
$[Ru_4H(CO)_{11}(dppb)BH_2]$	II	1150 (1 CO loss)	+106.6	+32.0 (1 P), −16.5 (1 P)	+7.6–7.0 (m, Ph), +3.7 (m, CH_2), +2.6–2.0 (m, CH_2), −8.0 (br, Ru–H–B), −8.6 (br, Ru–H–B), −21.2 (d, J_{PH} 2.3, Ru–H–Ru)
$[\{Ru_4H(CO)_{11}BH_2\}_2$(μ-dppb)]	II	1875	+106.7	+31.8	+7.6–7.0 (m, Ph), +3.7 (m, CH_2), +2.6–2.0 (m, CH_2), −8.0 (br, Ru–H–B), −8.8 (br, Ru–H–B), −21.2 (no coupling resolved, Ru–H–Ru)
$[Ru_4H(CO)_{11}(dpph)BH_2]$	II	1180	+106.4	+32.3 (1 P), −17.2 (1 P)	+7.6–7.0 (m, Ph), +4.1 (m, CH_2), +2.3 (m, CH_2), −7.9 (br, Ru–H–B), −8.6 (br, Ru–H–B), −21.2 (no coupling resolved, Ru–H–Ru)
$[\{Ru_4H(CO)_{11}BH_2\}_2$(μ-dpph)]	II	1905 (12 CO losses)	+106.4	+32.0	+7.6–7.0 (m, Ph), +4.2 (m, CH_2), +2.3 (m, CH_2), −8.0 (br, Ru–H–B), −8.7 (br, Ru–H–B), −21.3 (no coupling resolved, Ru–H–Ru)
$[Ru_4H(CO)_{11}(dppf)BH_2]$	I and II	1296 (P^+ + O) (11 CO losses)	+107.1	+33.4 (1 P), −20.1 (1 P)	+7.5–7.2 (m, Ph), +4.4–4.1 (br, C_5H_4), −7.7 (br, Ru–H–B), −8.6 (br, Ru–H–B), −21.2 (d, J_{PH} 2.3, Ru–H–Ru)
$[Ru_4H(CO)_{10}(dppf)BH_2]$	II	1228 (P^+ − CO) (9 CO losses)	+107.7	+46.5	+7.4–7.0 (m, Ph), +4.9 (2 H, C_5H_4), +4.4 (2 H, C_5H_4), +4.0 (2 H, C_5H_4), +3.7 (2 H, C_5H_4), −6.9 (br, Ru–H–B), −8.2 (br, Ru–H–B), −21.6 (t, J_{PH} 4, Ru–H–Ru)

Table 1 (*continued*)

Compound	Method of preparation[a]	Mass spectrometric data, m/z for P^+	NMR (δ, J/Hz) ^{11}B-{^1H}[b]	^{31}P[c]	^1H[d]
$[\{Ru_4H(CO)_{11}BH_2\}_2(\mu\text{-dppf})]$	I and II	2005 (11 CO losses)	+107.1	+33.4	+7.5–7.3 (m, Ph), +4.5–4.0 (br, C_5H_4), −7.3 (br, Ru–H–B), −8.0 (br, Ru–H–B), −21.1 (d, J_{PH} 2.3, Ru–H–Ru)
$[Ru_4H(CO)_{11}(dppa)BH_2]$	I and II	1136 (P^+ + O) (11 CO losses)	+107.1	+9.2 (1 P), −33.4 (1 P)	+7.8–7.2 (m, Ph), −7.8 (br, Ru–H–B), −8.7 (br, Ru–H–B), −21.2 (d, J_{PH} 2.6, Ru–H–Ru)
$[Ru_4H(CO)_{10}(dppa)_2BH_2]$	II	No parent ion (see text); 1090 (P^+ − dppa)	+106.0	+11.3, +9.0, −33.0 (2 isomers, see text)	+7.7–7.2 (m, Ph), −6.5 (br, Ru–H–B), −20.7 (no coupling resolved, Ru–H–Ru)
$[\{Ru_4H(CO)_{11}BH_2\}_2(\mu\text{-dppa})]$	I	1845 (4 CO losses)	+107.5	+12.1	+7.7–7.4 (m, Ph), −7.8 (br, Ru–H–B), −8.7 (br, Ru–H–B), −21.2 (d, J_{PH} 2.6, Ru–H–Ru)

[a] See Experimental section. [b] 128 MHz; with respect to δ 0 for $F_3B{\cdot}OEt_2$ (downfield shifts are positive); in $CDCl_3$ at 298 K. [c] 162 MHz; with respect to δ 0 for H_3PO_4 (downfield shifts are positive); in $CDCl_3$ at 298 K. [d] 250 or 400 MHz; with respect to δ 0 for $SiMe_4$ (downfield shifts are positive); d = doublet, t = triplet, br = broad, m = multiplet; in $CDCl_3$ at 298 K.

signatures of *cis*- and *trans*-$[Ru_4H(CO)_{10}(PPh_3)_2BH_2]$ are effectively the same; the boron atom and the hinge hydride cannot be significantly perturbed by the change in arrangement of the phosphorus-donor molecules. The signals for the Ru–H–B bridging H atoms are broadened by coupling to the boron nuclei and small changes in chemical shift are not readily observed. We were not able to separate the two isomers by chromatography and attempts at crystallisation were unsuccessful. The presence of both *cis* and *trans* isomers was also observed in $[Fe_4(CO)_{10}(PMe_2Ph)_2BH_2]^-$, but here intrasite exchange occurred on the NMR spectroscopic time-scale at 293 K.[7]

As expected, the carbonyl region of the IR spectrum of $[Ru_4H(CO)_{10}(PPh_3)_2BH_2]$ is shifted to lower wavenumbers than that of $[Ru_4H(CO)_{11}(PPh_3)BH_2]$ (Table 2) and the signatures of the two compounds are characteristic of the pattern of substitution if we compare these data with those of compounds described later.

The reaction between $[Ru_4H(CO)_{12}BH_2]$ and a two-fold excess of $P(C_6H_{11})_3$ yields $[Ru_4H(CO)_{11}\{P(C_6H_{11})_3\}BH_2]$ (≈25%) and $[Ru_4H(CO)_{10}\{P(C_6H_{11})_3\}_2BH_2]$ (≈20%) in addition to unreacted starting material. As for the PPh_3 derivatives, the ^{11}B NMR spectroscopic data indicate the retention of the cluster-core butterfly structure and boron environment upon mono- and di-substitution. Again, a loss and regain of symmetry in going from $[Ru_4H(CO)_{12}BH_2]$ to $[Ru_4H(CO)_{11}\{P(C_6H_{11})_3\}BH_2]$ to $[Ru_4H(CO)_{10}\{P(C_6H_{11})_3\}_2BH_2]$ is evidenced from the region of the ^1H NMR spectrum displaying the resonances for the Ru–H–B protons (Table 1). This, and the observed coupling (J_{PH} ≈3 Hz) to the hinge hydride, support wing-tip substitution in $[Ru_4H(CO)_{11}\{P(C_6H_{11})_3\}BH_2]$ and wing-tip–wing-tip disubstitution at different metal atoms in $[Ru_4H(CO)_{10}\{P(C_6H_{11})_3\}_2BH_2]$. The ^{31}P NMR spectrum of $[Ru_4H(CO)_{10}\{P(C_6H_{11})_3\}_2BH_2]$ exhibits only one signal indicating the preference for only one isomer, *cis* or *trans*. On steric grounds we propose that $[Ru_4H(CO)_{10}\{P(C_6H_{11})_3\}_2BH_2]$ exists as the *trans* isomer (substitution at sites 4 and 10 in Fig. 1); the cone angle for $P(C_6H_{11})_3$ is 170° compared with 145° for PPh_3.[21] The possible interconversion of *trans* and *cis* isomers is ruled out on the grounds that exchange does not occur at 298 K in the *less* sterically demanding PPh_3 analogue.

Crystal Structure of $[Ru_4H(CO)_{11}(PPh_3)BH_2]$.—Orange crystals of $[Ru_4H(CO)_{11}(PPh_3)BH_2]$, suitable for X-ray analysis, were grown at −20 °C from a CH_2Cl_2 solution layered with hexane. The structure is shown in Fig. 2, and selected bond distances and angles are listed in Table 5. The butterfly structure of the Ru_4 core is retained and the internal dihedral angle of the metal framework is 113.4° compared with 118° in the all-carbonyl cluster.[2] The PPh_3 ligand occupies one of the equatorial wing-tip ruthenium sites [Ru(4)–P 2.354(2) Å] and the Ru_4B core is perturbed very little by its presence. The three cluster hydrogen atoms have been located crystallographically and their positions bridging edges Ru(4)–B, Ru(1)–B and Ru(2)–Ru(3) are consistent with the ^1H NMR spectroscopic data discussed above.

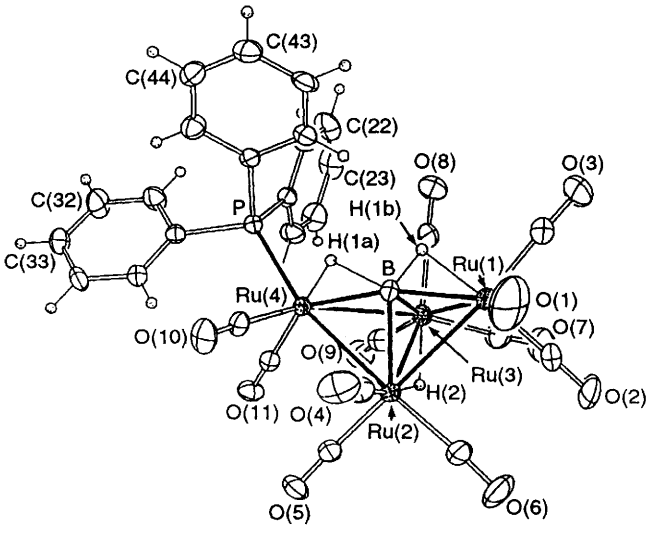

Fig. 2 Molecular structure of $[Ru_4H(CO)_{11}(PPh_3)BH_2]$

Substitution by a Ligand with a Small Cone Angle.—Relatively high degrees of substitution by small phosphine and phosphite ligands including $P(OMe)_3$ are well documented,[22] and in the reaction of $[Ru_4H(CO)_{12}BH_2]$ with $P(OMe)_3$ we used a large excess of phosphite (Tolman cone angle = 107°) to encourage the formation of $[Ru_4H(CO)_{12-x}\{P(OMe)_3\}_xBH_2]$ with relatively high values of x, thereby allowing us to probe the third and fourth sites of substitution on the butterfly framework. The reaction of $[Ru_4H(CO)_{12}BH_2]$ with a 30-fold excess of $P(OMe)_3$ leads to the formation of $[Ru_4H$-

Table 2 Infrared spectroscopic data for products from the reactions of $[Ru_4H(CO)_{12}BH_2]$ with PPh_3, $P(C_6H_{11})_3$, $P(OMe)_3$, dppe, dppp, dppb, dpph, dppf and dppa

Compound	$\tilde{\nu}$(CO) (CH_2Cl_2)/cm^{-1}
$[Ru_4H(CO)_{11}(PPh_3)BH_2]$	2088m, 2050vs, 2022m, 2013m
$[Ru_4H(CO)_{10}(PPh_3)_2BH_2]$	2064m, 2039vs, 2016vs, 1990vs
$[Ru_4H(CO)_{11}\{P(C_6H_{11})_3\}BH_2]$	2073w, 2047vs, 2019m, 2005m
$[Ru_4H(CO)_{10}\{P(C_6H_{11})_3\}_2BH_2]$	2058m, 2030vs, 2006vs, 1978vs
trans-$[Ru_4H(CO)_{10}\{P(OMe)_3\}_2BH_2]$	2070m, 2042vs, 2023s, 1994s
cis-$[Ru_4H(CO)_{10}\{P(OMe)_3\}_2BH_2]$	2075w, 2041vs, 2027s, 2006s
$[Ru_4H(CO)_9\{P(OMe)_3\}_3BH_2]$	2055w, 2016vs, 1985m
$[Ru_4H(CO)_8\{P(OMe)_3\}_4BH_2]$	2065w, 2021m, 2003s, 1995vs, 1965m
$[Ru_4H(CO)_{10}(dppe)BH_2]$	2075m, 2043vs, 2010m, 1995m
$[\{Ru_4H(CO)_{11}BH_2\}_2(\mu\text{-dppe})]$	2089m, 2052vs, 2023m, 2012m, 1988m
$[Ru_4H(CO)_{11}(dppp)BH_2]$	2088m, 2052vs, 2025s, 2015m, 2001m
$[Ru_4H(CO)_{10}(dppp)BH_2]$	2075m, 2037vs, 2007m, 1985w
$[\{Ru_4H(CO)_{11}BH_2\}_2(\mu\text{-dppp})]$	2086m, 2058vs, 2020s, 2012m, 2000m
$[Ru_4H(CO)_{11}(dppb)BH_2]$	2089w, 2051vs, 2025m, 2014m
$[\{Ru_4H(CO)_{11}BH_2\}_2(\mu\text{-dppb})]$	2088m, 2051vs, 2024m, 2012m
$[Ru_4H(CO)_{11}(dpph)BH_2]$	2089m, 2052vs, 2023m, 2012m, 1988m
$[\{Ru_4H(CO)_{11}BH_2\}_2(\mu\text{-dpph})]$	2087w, 2050vs, 2022m, 2011m
$[Ru_4H(CO)_{11}(dppf)BH_2]$	2088m, 2052vs, 2024m, 2015m, 1993w
$[Ru_4H(CO)_{10}(dppf)BH_2]$	2078m, 2042vs, 2020s, 1990m
$[\{Ru_4H(CO)_{11}BH_2\}_2(\mu\text{-dppf})]$	2089m, 2054vs, 2026m, 2016m, 1994w
$[Ru_4H(CO)_{11}(dppa)BH_2]$	2089w, 2053vs, 2027m, 2018m, 1995w
$[Ru_4H(CO)_{10}(dppa)_2BH_2]$	2067m, 2041vs, 2022s, 1993s
$[\{Ru_4H(CO)_{11}BH_2\}_2(\mu\text{-dppa})]$	2090m, 2055vs, 2028s, 2019s, 2007m

$(CO)_{10}\{P(OMe)_3\}_2BH_2]$ (≈15%), $[Ru_4H(CO)_9\{P(OMe)_3\}_3BH_2]$ (≈40%) and $[Ru_4H(CO)_8\{P(OMe)_3\}_4BH_2]$ (≈30%) as the major products, and no *mono*substituted derivative was obtained. The chemical shift of the ^{11}B NMR resonance (Table 1) of each of these compounds is consistent with there being little perturbation of the boron environment upon phosphite substitution.

The ^{31}P NMR spectrum of $[Ru_4H(CO)_{10}\{P(OMe)_3\}_2BH_2]$ exhibits two signals at 298 K (δ +144.8 and +143.6) in an approximately 1:1 ratio. These data do not distinguish between the presence of two isomers or the presence of a single compound with two different phosphorus environments. In contrast to failed attempts to separate the isomers of $[Ru_4H(CO)_{10}(PPh_3)_2BH_2]$, separation of *cis*- and *trans*-$[Ru_4H(CO)_{10}\{P(OMe)_3\}_2BH_2]$ was achieved by thin-layer chromatography (reseparation of the initial sample eluting with CH_2Cl_2–hexane 3:2) or by recrystallisation (see below). The ^{31}P NMR spectrum of each isomer exhibits only one signal (Table 1). The ^1H NMR spectra of *cis*- and *trans*-$[Ru_4H(CO)_{10}\{P(OMe)_3\}_2BH_2]$ are similar. In the high-field region a broad signal at δ −8.4 (*trans*) or δ −8.1 (*cis*) can be assigned to the two equivalent Ru–H–B hydrogen atoms and confirms symmetrical wing-tip–wing-tip substitution patterns. Each isomer exhibits a triplet resonance for the Ru–H–Ru hydride with J_{PH} 3 Hz. These data are similar to those of both $[Ru_4H(CO)_{10}(PPh_3)_2BH_2]$ and $[Ru_4H(CO)_{10}\{P(C_6H_{11})_3\}_2BH_2]$. The crystal structure of *trans*-$[Ru_4H(CO)_{10}\{P(OMe)_3\}_2BH_2]$ has been determined and is described below.

The cluster $[Ru_4H(CO)_9\{P(OMe)_3\}_3BH_2]$ provides us with the first example of substitution at a site other than a wing-tip ruthenium atom. Once again the ^{11}B NMR resonance indicates retention of the butterfly skeleton around the boron centre. The ^{31}P NMR spectrum shows two signals in a ratio 2:1 with almost identical shifts (Table 1). The most useful indicators of structure in the ^1H NMR spectrum of $[Ru_4H(CO)_9\{P(OMe)_3\}_3BH_2]$ are again the signals due to the Ru–H–B and Ru–H–Ru hydrogen atoms. The presence of broad signals centred at δ −8.6 and −9.0 indicates that the symmetry of the parent carbonyl cluster has been broken. The hydride at δ −21.3 is a doublet of triplets, with respective couplings of J_{PH} 5 and 2 Hz. The latter reflects the coupling seen for the disubstituted derivatives described above whilst the former is characteristic of a two-bond *cis* coupling. Substitution at a hinge-metal site with a *cis* H–Ru–P arrangement has been observed in $[FeRu_3H(CO)_{10}\{P(OMe)_3\}_2N]$; here the second ligand is in a wing-tip (Ru) site and the signal for the Ru–H–Ru hinge hydride appears as a doublet (J_{PH} 8.5 Hz) of doublets (J_{PH} 1.4 Hz).[11]

Possible substitution patterns in $[Ru_4H(CO)_9\{P(OMe)_3\}_3BH_2]$ which would be consistent with the spectroscopic data are (see Fig. 1) [4,7,10], [4,9,12] or [4,9,10]. None of these patterns permits the two wing-tip P atoms to be chemically equivalent and we must therefore assume that the ^{31}P NMR resonance of intensity two arises because of the (not unreasonable) coincidence of signals. Of the three possible structures we favour a [4,7,10] pattern on steric grounds. This would give a 'paddle-wheel' arrangement for the three ligands around the periphery of the butterfly core.

The ^1H NMR spectrum of the tetrasubstituted product indicates that a degree of symmetry has been restored to the compound; there is only one Ru–H–B environment (Table 1). Two resonances are observed in the ^{31}P NMR spectrum (equal intensities) and the ^1H NMR spectroscopic signal for the Ru–H–Ru hinge hydride is a triplet of triplets with couplings of J_{PH} 4 and 8 Hz. These data indicate that the fourth ligand enters in a site that completes the pattern set in the trisubstituted cluster, and gives a [1,4,7,10] substitution pattern. Conversely, the assignment of a structure for $[Ru_4H(CO)_8\{P(OMe)_3\}_4BH_2]$ gives supporting evidence for the proposed structure of $[Ru_4H(CO)_9\{P(OMe)_3\}_3BH_2]$.

Crystal Structure of trans-$[Ru_4H(CO)_{10}\{P(OMe)_3\}_2BH_2]$.—Yellow crystals of *trans*-$[Ru_4H(CO)_{10}\{P(OMe)_3\}_2BH_2]$, suitable for X-ray analysis, were grown at −20 °C from a CH_2Cl_2 solution of both the *cis* and *trans* isomers which was layered with hexane. Its structure is shown in Fig. 3 and selected bond distances and angles are listed in Table 7. The retention of the butterfly core and the presence of the semiinterstitial boron atom are confirmed. The internal dihedral angle of the Ru_4 skeleton is 115.1°, a value that is similar to those both of $[Ru_4H(CO)_{12}BH_2]$[2] and $[Ru_4H(CO)_{11}(PPh_3)BH_2]$. Each $P(OMe)_3$ ligand is attached to a different wing-tip ruthenium atom [Ru(2) and Ru(4)] and the arrangement corresponds to a [4,10] pattern in terms of the numbering scheme in Fig. 1. The two ruthenium–phosphorus distances are similar [Ru(2)–P(2) 2.269(2) and Ru(4)–P(1) 2.272(3) Å]. Hydrogen atoms were not located but inspection of the carbonyl ligand orientations and consideration of the NMR spectroscopic data (see above) are consistent with their placement along the edges Ru(2)–B, Ru(4)–B and Ru(1)–Ru(3).

Table 3 Crystallographic data * for $[Ru_4H(CO)_{11}(PPh_3)BH_2]$, *trans*-$[Ru_4H(CO)_{10}\{P(OMe)_3\}_2BH_2]$ and $[Ru_4H(CO)_{10}(dppe)BH_2]\cdot CH_2Cl_2$

Formula	$C_{29}H_{18}BO_{11}PRu_4$	$C_{16}H_{20}BO_{16}P_2Ru_4$	$C_{37}H_{29}BCl_2O_{10}P_2Ru_4$
M	988.5	945.3	1181.5
Space group	$P2_1/c$	$P2_1/n$	$P2_1/n$
a/Å	14.099(3)	12.87(6)	14.723(4)
b/Å	14.088(4)	15.599(4)	15.519(4)
c/Å	17.707(4)	15.414(7)	18.608(5)
β/°	109.57(2)	98.98(2)	95.06(2)
U/Å^3	3313.9(14)	3044(2)	4235(2)
Crystal dimensions/mm	0.21 × 0.23 × 0.47	0.30 × 0.35 × 0.40	0.38 × 0.40 × 0.45
Crystal colour	Orange	Yellow	Orange
D_c/g cm^3	1.981	2.063	1.853
μ(Mo-Kα)/cm^{-1}	18.58	20.78	16.27
T/K	296	296	243
2θ scan range/°	4–50	4–55	4–55
Reflections collected	6032	7338	10011
Independent reflections	5828	6974	9721
Observed reflections $[F_o \geqslant n\sigma(F_o)]$	4012 (n = 4)	4422 (n = 5)	6025 (n = 5)
R	0.0408	0.0444	0.0482
R'	0.0494	0.0534	0.0594
Δ/σ (max)	0.105	0.124	0.242
Δ(ρ)/e Å^{-3}	0.59	0.88	1.22
N_o/N_v	9.2	12.6	11.7
Goodness of fit	1.03	1.11	1.28

* Details in common: monoclinic; Z = 4; Siemens P4 diffractometer, graphite-monochromated Mo-Kα radiation (λ = 0.710 73 Å); quantity minimized = $\Sigma w\Delta^2$; $R = \Sigma\Delta/\Sigma(F_o)$; $R' = \Sigma\Delta w^{\frac{1}{2}}/\Sigma(F_o w^{\frac{1}{2}})$, $\Delta = |F_o - F_c|$; N_o, N_v numbers of observations and variables.

Table 4 Atomic coordinates (× 10^4) for $[Ru_4H(CO)_{11}(PPh_3)BH_2]$

Atom	x	y	z	Atom	x	y	z
Ru(1)	5 228(1)	3 044(1)	6 465(1)	C(7)	4 571(7)	770(9)	6 185(6)
Ru(2)	6 017(1)	2 587(1)	5 231(1)	C(8)	6 347(6)	985(7)	7 484(5)
Ru(3)	5 932(1)	1 165(1)	6 365(1)	C(9)	6 359(7)	−36(8)	6 081(5)
Ru(4)	7 857(1)	1 860(1)	6 328(1)	C(10)	8 663(5)	2 716(6)	5 984(4)
P	9 155(1)	1 284(1)	7 455(1)	C(11)	8 000(5)	855(5)	5 648(4)
B	6 659(6)	2 538(7)	6 544(5)	C(21)	8 957(6)	318(7)	8 812(5)
O(1)	5 105(7)	5 178(8)	6 229(7)	C(22)	8 721(8)	−467(8)	9 182(6)
O(2)	3 094(5)	2 606(9)	5 390(5)	C(23)	8 408(8)	−1 279(8)	8 766(7)
O(3)	4 539(6)	3 078(9)	7 924(4)	C(24)	8 298(7)	−1 328(7)	7 940(6)
O(4)	6 886(6)	4 540(5)	5 168(4)	C(25)	8 529(6)	−536(6)	7 586(5)
O(5)	6 804(5)	1 783(5)	3 958(3)	C(26)	8 850(5)	286(5)	7 996(4)
O(6)	3 913(5)	3 050(6)	4 059(4)	C(31)	10 953(6)	250(6)	7 861(5)
O(7)	3 786(6)	498(8)	6 105(5)	C(32)	11 859(7)	−23(7)	7 779(6)
O(8)	6 590(5)	904(6)	8 165(4)	C(33)	12 148(6)	307(6)	7 163(5)
O(9)	6 558(5)	−771(5)	5 908(4)	C(34)	11 504(6)	903(6)	6 601(5)
O(10)	9 064(4)	3 287(4)	5 760(4)	C(35)	10 592(5)	1 180(6)	6 669(4)
O(11)	8 098(4)	268(4)	5 252(3)	C(36)	10 314(5)	862(5)	7 301(4)
C(1)	5 117(8)	4 380(10)	6 310(7)	C(41)	8 899(6)	2 676(6)	8 499(4)
C(2)	3 891(7)	2 759(11)	5 796(6)	C(42)	9 214(6)	3 368(6)	9 071(4)
C(3)	4 818(7)	3 038(9)	7 380(6)	C(43)	10 213(7)	3 627(6)	9 368(5)
C(4)	6 545(7)	3 826(8)	5 181(5)	C(44)	10 900(6)	3 174(6)	9 120(5)
C(5)	6 526(6)	2 081(6)	4 447(5)	C(45)	10 618(6)	2 457(6)	8 547(5)
C(6)	4 678(7)	2 883(7)	4 508(5)	C(46)	9 599(5)	2 211(5)	8 227(4)

Ligands with Two P-*Donor Atoms*.—The use of a diphosphine provides four possible modes of interaction with the cluster $[Ru_4H(CO)_{12}BH_2]$: (1) chelate at one Ru, (2) edge bridging two Ru atoms, (3) monodentate (pendant) and (4) linkage between two clusters; these are summarised in Fig. 4. In this study we have included ligands with flexible backbones (dppe, dppp, dppb, dpph and dppf) and one (dppa) with a rigid backbone.

The reaction between $[Ru_4H(CO)_{12}BH_2]$ and dppe leads to the formation of the yellow compounds $[Ru_4H(CO)_{10}(dppe)BH_2]$ (≈20%) and $[\{Ru_4H(CO)_{11}BH_2\}_2(\mu\text{-dppe})]$ (≈10%) in addition to unreacted starting material. The carbonyl region of the IR spectra of the products is quite instructive, but not definitive, as to the pattern of substitution. The spectral signature for a product of either the pendant or linked type is expected to resemble that of a monosubstituted cluster and indeed the IR spectrum around 2000 cm^{-1} of one product of the reaction bears a close resemblance to that of $[Ru_4H(CO)_{11}(PPh_3)BH_2]$. The mass spectrum of the product shows a parent ion in agreement with a formulation of $[\{Ru_4H(CO)_{11}BH_2\}_2(\mu\text{-dppe})]$. The ^{11}B NMR resonance (Table 1) indicates that no perturbation of the cluster framework has occurred upon substitution, and the appearance of only one signal indicates that the boron environments in the two sub-clusters are equivalent. In the high-field region of the ^{1}H NMR spectrum the signal assigned to the hinge hydride is a doublet (J_{PH} 2.3 Hz). Again, the appearance of *one* signal supports equivalence of the two sub-clusters, and the coupling is characteristic of wing-tip substitution as described above for $[Ru_4H(CO)_{11}(PPh_3)BH_2]$ and related species. Although two Ru–H–B environments are expected only one very broad signal ($w_{\frac{1}{2}}$ = 375 Hz) is observed. The presence in the ^{31}P NMR spectrum of one resonance is also consistent with the proposed structure; the chemical shift is δ +34.1, shifted downfield with respect to the free diphosphine (δ −13.5).

A formulation of $[Ru_4H(CO)_{10}(dppe)BH_2]$ for the second product of the reaction was initially supported by mass spectrometric data (Table 1). The ^{11}B NMR spectrum shows two signals (δ +107 and +112, ratio 3:2), both close to that of the precursor and indicating (*i*) the presence of two isomers of $[Ru_4H(CO)_{10}(dppe)BH_2]$ and (*ii*) the retention in each isomer of the butterfly cluster framework. The ^{31}P NMR spectrum is consistent with the formation of two isomers; four signals are observed in a ratio 3:2:3:2 (δ +47.9, +43.4, +40.0 and +39.1 respectively) and these chemical shifts are all typical of *co-ordinated* PPh_2 groups. The presence of two phosphorus environments per isomer suggests that in each the dppe ligand is edge bridging rather than chelating. Once again we are able to use the coupling between the ^{31}P nuclei and the Ru–H–Ru hinge hydride to gain information about the exact sites of substitution. In the ^{31}P NMR spectrum the signal at δ +39.1 is a well resolved doublet (J_{PH} = 36 Hz) indicative of a *trans* H–Ru–P arrangement, *i.e.* substitution at a hinge site (2 or 8, Fig. 1). The metal hydride region of the ^1H NMR spectrum can be interpreted in terms of two overlapping doublets of doublets, and the coupling constants (Table 1) are consistent with a substitution pattern of [2,4] or [2,6] in one isomer and [3,4] or [3,6] in the second isomer. The two possibilities [2,6] and [3,6] can be ruled out after consideration of the bite size of dppe.

We have not been able to separate the two isomers of $[Ru_4H(CO)_{10}(dppe)BH_2]$ by chromatography, but X-ray-quality crystals of one isomer were grown (−20 °C) from a mixture of the isomers in CH_2Cl_2 layered with hexane. The structure of $[Ru_4H(CO)_{10}(dppe)BH_2]$ is shown in Fig. 5, and selected bond distances and angles are listed in Table 9. The results confirm that the boron-containing butterfly core has been retained. The internal dihedral angle of the metal framework is 115.1°, the same as in *trans*-$[Ru_4H(CO)_{10}\{P(OMe)_3\}_2BH_2]$. The dppe ligand bridges the edge Ru(1)–Ru(3), with one phosphorus atom occupying an equatorial site of wing-tip atom Ru(3) and the other residing in an axial site of hinge atom Ru(1). These sites confirm a [2,4] pattern of substitution for one of the isomers. The cluster hydrogen atoms have been located crystallographically and the positions bridging edges Ru(1)–Ru(2), Ru(3)–B and Ru(4)–B are consistent with the NMR spectroscopic data (see above).

Having established the way in which dppe reacts with $[Ru_4H(CO)_{12}BH_2]$, we turned our attention to the effects of increasing the length of the carbon backbone of the ligand $Ph_2P(CH_2)_nPPh_2$ and studied the reactions of the diphosphines dppp (n = 3), dppb (n = 4) and dpph (n = 6) with $[Ru_4H(CO)_{12}BH_2]$. We have already noted that the products of reactions between these ligands and $Na_2[PdCl_4]$ are dependent upon the nature of the diphosphine; monomeric complexes $[PdCl_2(dppe)]$, $[PdCl_2(dppp)]$ and $[PdCl_2(dppb)]$ form, but a dinuclear species *trans*-$[Pd_2Cl_4(\mu\text{-dpph})_2]$ is produced when the carbon backbone is longer.[23]

A preliminary reaction in which a CH_2Cl_2 solution of dppp and $[Ru_4H(CO)_{12}BH_2]$ was stirred at room temperature for 8 d produced the yellow compounds $[Ru_4H(CO)_{11}(dppp)BH_2]$ (≈20%) and $[\{Ru_4H(CO)_{11}BH_2\}_2(\mu\text{-dppp})]$ (≈30%) in addition to unreacted $[Ru_4H(CO)_{12}BH_2]$. These products were spectroscopically characterised; over a period of hours standing in CH_2Cl_2 solution $[Ru_4H(CO)_{11}(dppp)BH_2]$ converts into $[\{Ru_4H(CO)_{11}BH_2\}_2(\mu\text{-dppp})]$. The carbonyl regions of the IR spectra of these two compounds are extremely similar, as are the ^{11}B and ^1H NMR spectroscopic signatures. These observations are consistent with the ligands adopting a pendant and a linked mode of attachment (Fig. 4). Mass spectrometric data (Table 1) support the proposal of the linked product $[\{Ru_4H(CO)_{11}BH_2\}_2(\mu\text{-dppp})]$, but the parent ion in the mass spectrum of the second product corresponded to $[P^+ + O]$. We have noted the apparent oxidation of the non-co-ordinated PPh_2 group during attempts to gain mass spectrometric data for several members of this group of compounds, but ^{31}P NMR spectroscopic data confirm that this does not appear to be a problem in solution. The ^{31}P NMR spectrum of $[\{Ru_4H(CO)_{11}BH_2\}_2(\mu\text{-dppp})]$ shows one reso-

Table 5 Selected bond distances (Å) and angles (°) for $[Ru_4H(CO)_{11}(PPh_3)BH_2]$

Ru(1)–Ru(2)	2.839(1)	Ru(1)–Ru(3)	2.853(1)
Ru(2)–Ru(3)	2.867(1)	Ru(2)–Ru(4)	2.860(1)
Ru(3)–Ru(4)	2.906(1)	Ru(1)–B	2.100(9)
Ru(2)–B	2.196(8)	Ru(3)–B	2.161(9)
Ru(4)–B	2.084(9)	Ru(4)–P	2.354(2)
Ru(2)–Ru(1)–Ru(3)	60.5(1)	Ru(1)–Ru(2)–Ru(3)	60.0(1)
Ru(1)–Ru(2)–Ru(4)	93.3(1)	Ru(3)–Ru(2)–Ru(4)	61.0(1)
Ru(1)–Ru(3)–Ru(2)	59.5(1)	Ru(1)–Ru(3)–Ru(4)	92.1(1)
Ru(2)–Ru(3)–Ru(4)	59.4(1)	Ru(2)–Ru(4)–Ru(3)	59.6(1)
Ru(2)–Ru(4)–P	166.0(1)	Ru(3)–Ru(4)–P	109.4(1)
Ru(2)–Ru(1)–B	50.1(2)	Ru(1)–Ru(2)–B	47.2(2)
Ru(3)–Ru(2)–B	48.3(2)	Ru(4)–Ru(2)–B	46.4(2)
Ru(1)–Ru(3)–B	47.0(2)	Ru(2)–Ru(3)–B	49.4(2)
Ru(4)–Ru(3)–B	45.7(2)	Ru(3)–Ru(4)–B	47.9(2)
Ru(2)–Ru(4)–B	49.8(2)	Ru(3)–Ru(1)–B	48.9(2)
Ru(2)–B–Ru(3)	82.3(3)	Ru(1)–B–Ru(4)	164.4(4)
B–Ru(4)–P	116.8(2)		

Table 6 Atomic coordinates (× 10^4) for *trans*-$[Ru_4H(CO)_{10}\{P(OMe)_3\}_2BH_2]$

Atom	x	y	z	Atom	x	y	z
Ru(1)	−631(1)	6451(1)	1526(1)	O(14)	1208(8)	3956(5)	2725(8)
Ru(2)	514(1)	5943(1)	3186(1)	O(15)	1955(7)	5014(4)	1912(5)
Ru(3)	−1145(1)	7174(1)	3131(1)	O(16)	2615(7)	4834(7)	3474(7)
Ru(4)	−2638(1)	6122(1)	2033(1)	C(1)	734(7)	6762(6)	1270(5)
P(1)	−3983(2)	6029(2)	2830(2)	C(2)	−640(7)	5342(6)	1024(5)
P(2)	1596(2)	4902(1)	2812(2)	C(3)	−1408(7)	7055(6)	555(5)
B	−1096(6)	5842(6)	2702(5)	C(4)	1596(6)	6760(5)	3132(5)
O(1)	1515(5)	6938(5)	1053(5)	C(5)	876(7)	5760(5)	4415(5)
O(2)	−682(6)	4669(4)	727(4)	C(6)	−46(7)	7920(5)	3698(6)
O(3)	−1821(6)	7439(5)	−19(4)	C(7)	−1538(7)	6793(7)	4193(6)
O(4)	2264(5)	7239(4)	3083(4)	C(8)	−2236(7)	8023(5)	2915(6)
O(5)	1059(6)	5633(5)	5154(4)	C(9)	−3305(7)	7057(5)	1387(6)
O(6)	560(6)	8391(5)	4039(5)	C(10)	−3178(7)	5317(5)	1161(5)
O(7)	−1783(7)	6558(6)	4817(5)	C(11)	−4876(11)	6968(9)	3947(8)
O(8)	−2871(6)	8541(4)	2842(5)	C(12)	−5606(8)	5929(9)	1558(8)
O(9)	−3707(6)	7618(4)	998(4)	C(13)	−3561(10)	4609(8)	3712(9)
O(10)	−3485(6)	4829(5)	637(4)	C(14)	474(10)	3531(7)	3051(9)
O(11)	−4095(6)	6839(5)	3398(5)	C(15)	2168(10)	4423(9)	1306(8)
O(12)	−5116(7)	5873(11)	2372(6)	C(16)	3338(11)	4373(14)	3663(12)
O(13)	−3955(10)	5327(6)	3549(9)				

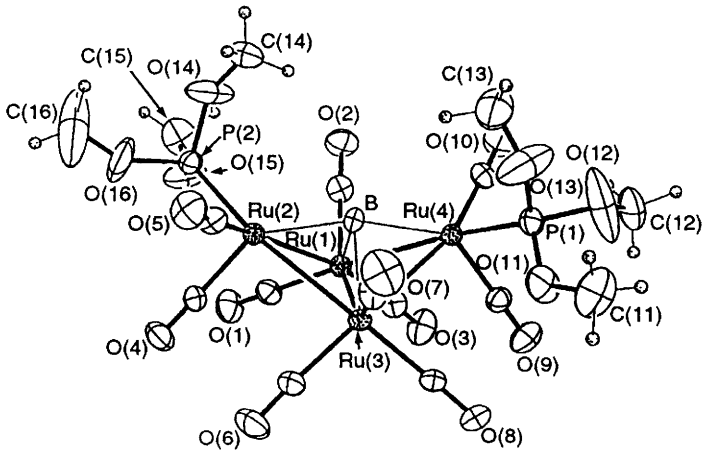

Fig. 3 Molecular structure of *trans*-$[Ru_4H(CO)_{10}\{P(OMe)_3\}_2BH_2]$. Cluster hydrogen atoms were not located

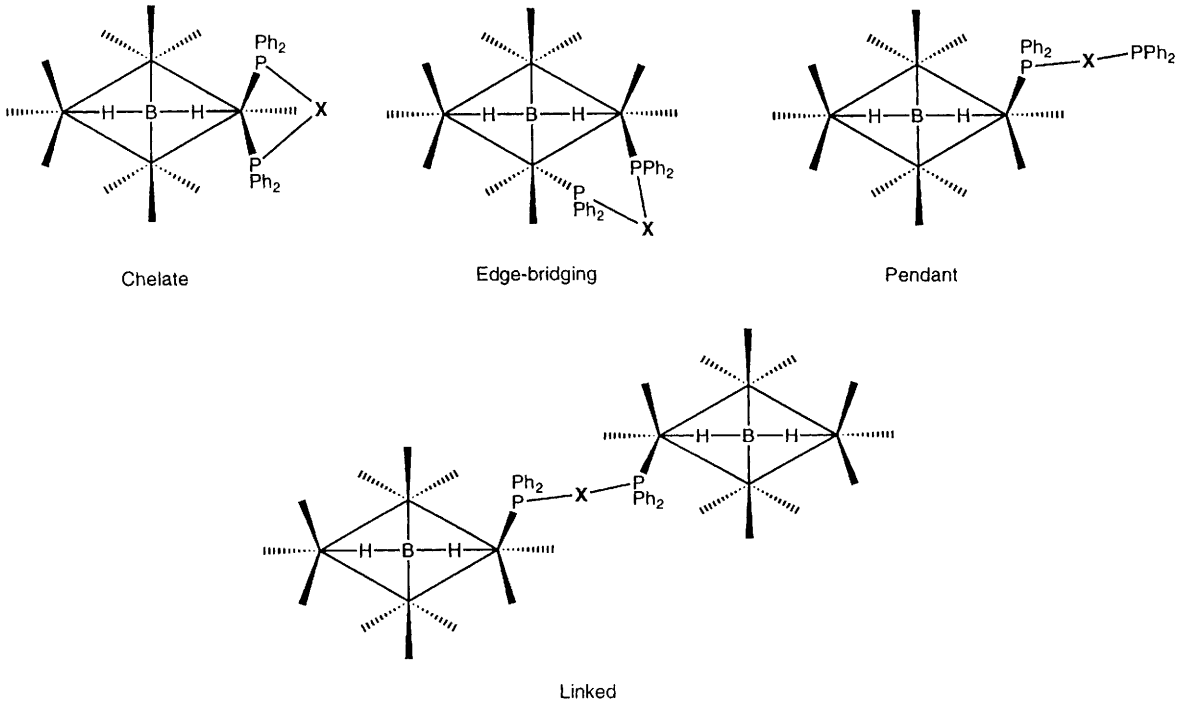

Fig. 4 The four general modes of substitution for a diphosphine Ph_2PXPPh_2 (see text for X) when it reacts with the cluster $[Ru_4H(CO)_{12}BH_2]$. Isomers are possible for each of the structures

nance, the shift of which (δ +31.4) is typical of a co-ordinated phosphine. In contrast, the spectrum of $[Ru_4H(CO)_{11}(dppp)BH_2]$ exhibits two resonances (1:1), one with a shift (δ +33.2) consistent with a co-ordinated PPh_2 group, and one with a shift (δ −17.9) close to that of free dppp (δ −18.5).

When the reaction of dppp with $[Ru_4H(CO)_{12}BH_2]$ is repeated under the conditions of method II (photolysis and a two-fold excess of dppp), three products are obtained in addition to unreacted starting cluster. These are $[Ru_4H(CO)_{11}(dppp)BH_2]$ (≈15%), $[\{Ru_4H(CO)_{11}BH_2\}_2(\mu\text{-dppp})]$ (≈5%) and $[Ru_4H(CO)_{10}(dppp)BH_2]$ (≈20%). The spectroscopic properties of the final product are listed in Tables 1 and 2 and are consistent with the dppp ligand adopting a chelating mode (Fig. 4). The ^1H and ^{31}P NMR spectra in particular reveal features that distinguish $[Ru_4H(CO)_{10}(dppp)BH_2]$ from $[Ru_4H(CO)_{11}(dppp)BH_2]$. For the former only one ^{31}P NMR signal is observed (δ +32.3) indicating the co-ordination of both P-donor atoms to the cluster. Further evidence that the two substitution sites are equivalent and that the mode is chelating rather than edge bridging comes from the resonance for the Ru–H–Ru hydride in the ^1H NMR spectrum. This is a triplet (J_{PH} 2.3 Hz) and shows that both PPh_2 groups are attached to wing-tip ruthenium sites. The ligand is too short to bridge over the top of the cluster and thus a [4,12]- or [4,10]-substitution pattern can be ruled out. Additionally, the two broad signals at δ −7.3 and −8.6 assigned to the Ru–H–B protons confirm the non-equivalence of the two wing-tip ruthenium atoms and the presence of a [4,6] substitution pattern. Note too that in going from $[Ru_4H(CO)_{12}BH_2]$ to $[Ru_4H(CO)_{11}(dppp)BH_2]$ to $[Ru_4H(CO)_{10}(dppp)BH_2]$ the shift of the signals for one of the two Ru–H–B protons is significantly affected by the presence of the phosphine ligands as shown in Fig. 6.

The ligands dppb and dpph (L–L) react with $[Ru_4H(CO)_{12}BH_2]$ to form both $[Ru_4H(CO)_{11}(L\text{–}L)BH_2]$ and $[\{Ru_4H(CO)_{11}BH_2\}_2(\mu\text{-L–L})]$ but no product in which the ligand is in a chelating mode. For dppb, the linked product predominates {yield ≈45% *versus* ≈10% of $[Ru_4H(CO)_{11}(dppb)BH_2]$}, but in the case of dpph the reaction gave only ≈10% of each product after a 17 h reaction period. Unreacted $[Ru_4H(CO)_{12}BH_2]$ was recovered as the third component of the final mixture in each reaction. Spectroscopic

data for $[Ru_4H(CO)_{11}(dppb)BH_2]$, $[\{Ru_4H(CO)_{11}BH_2\}_2(\mu\text{-dppb})]$, $[Ru_4H(CO)_{11}(dpph)BH_2]$ and $[\{Ru_4H(CO)_{11}BH_2\}_2(\mu\text{-dpph})]$ are collected in Tables 1 and 2 and the same arguments as in the discussion of the dppp derivatives can be applied to support the proposals that both the dppb and dpph ligands show a preference for the pendant or linked over chelating or edge-bridging modes of attachment.

Reactions with dppf. It is now well established that dppf is flexible and can co-ordinate to mononuclear metal centres,[12–18] bridge dimetallic frameworks[24] and bind to clusters[25] in chelating, pendant, edge-bridging and linking modes. An instructive example is $[W_2H(CO)_8(NO)(dppf)]$ which has been crystallographically characterised. The ligand adopts a monodentate (pendant) co-ordination mode although the reaction of $[W_2H(CO)_9(NO)]$ with dppf also produces $[W_2H(CO)_7(NO)(dppf)]$ and $[\{W_2H(CO)_8(NO)\}_2(\mu\text{-dppf})]$.[17] The reaction of $[Ru_3(CO)_{12}]$ with dppf produces $[Ru_3(CO)_{10}(dppf)]$ in which the ligand bridges a Ru–Ru edge, although a change in the reaction conditions permits the formation of $[Ru_3(CO)_8(dppf)_2]$.[25a] The compound $[Ru_4H_4(CO)_{12}]$ reacts with dppf to yield $[Ru_4H_4(CO)_{10}(dppf)]$.[25a] The cluster $[Ru_4H(CO)_{12}BH_2]$ offers the possibility of all the four modes of attachment illustrated in Fig. 4.

The pattern of reaction of $[Ru_4H(CO)_{12}BH_2]$ with dppf proved to be similar to that with dppp. When a CH_2Cl_2 solution of dppf and $[Ru_4H(CO)_{12}BH_2]$ was stirred at room temperature for 8 d, thin-layer chromatography revealed the presence of twelve fractions, but only three were present in large enough quantity to be isolated. The first was $[Ru_4H_4(CO)_{12}]$ ($\approx$10%).[1] The yellow compounds $[Ru_4H(CO)_{11}(dppf)BH_2]$ and $[\{Ru_4H(CO)_{11}BH_2\}_2(\mu\text{-dppf})]$ were typically produced in

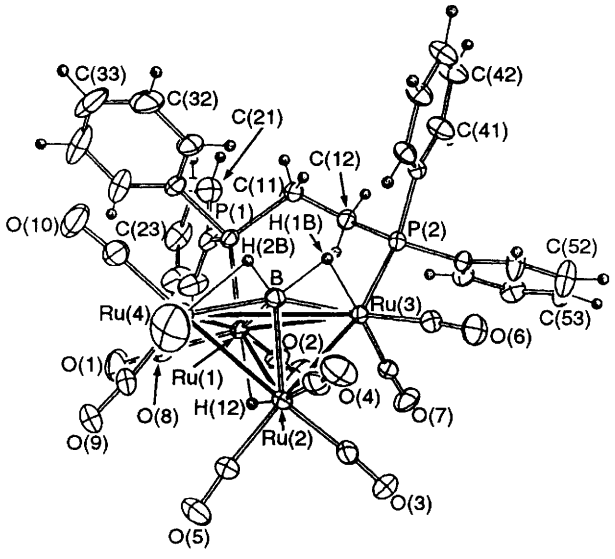

Fig. 5 Molecular structure of $[Ru_4H(CO)_{10}(dppe)BH_2]$

Table 7 Selected bond distances (Å) and angles (°) for *trans*-$[Ru_4H(CO)_{10}\{P(OMe)_3\}_2BH_2]$

Ru(1)–Ru(2)	2.856(1)	Ru(1)–Ru(3)	2.887(1)
Ru(2)–Ru(3)	2.856(1)	Ru(1)–Ru(4)	2.849(1)
Ru(3)–Ru(4)	2.866(1)	Ru(1)–B	2.208(9)
Ru(2)–B	2.088(8)	Ru(3)–B	2.185(9)
Ru(4)–B	2.127(8)	Ru(2)–P(2)	2.269(2)
Ru(4)–P(1)	2.272(3)		
Ru(2)–Ru(1)–Ru(3)	59.7(1)	Ru(2)–Ru(1)–Ru(4)	93.7(1)
Ru(3)–Ru(1)–Ru(4)	59.9(1)	Ru(1)–Ru(2)–Ru(3)	60.7(1)
Ru(1)–Ru(3)–Ru(2)	59.6(1)	Ru(1)–Ru(3)–Ru(4)	59.4(1)
Ru(2)–Ru(3)–Ru(4)	93.3(1)	Ru(3)–Ru(2)–P(2)	162.9(1)
Ru(1)–Ru(2)–P(2)	102.7(1)	Ru(3)–Ru(4)–P(1)	102.1(1)
Ru(1)–Ru(4)–P(1)	162.4(1)	Ru(4)–Ru(1)–B	47.7(2)
Ru(2)–Ru(1)–B	46.6(2)	Ru(3)–Ru(2)–B	49.5(2)
Ru(1)–Ru(2)–B	50.2(2)	Ru(3)–Ru(4)–B	49.2(2)
Ru(1)–Ru(3)–B	49.3(2)	Ru(2)–Ru(3)–B	46.6(2)
Ru(4)–Ru(3)–B	47.5(2)	Ru(3)–Ru(1)–B	48.6(2)
Ru(1)–Ru(4)–B	50.1(2)	Ru(2)–B–Ru(4)	161.8(5)
Ru(1)–B–Ru(3)	82.2(3)	B–Ru(2)–P(2)	117.7(2)
B–Ru(4)–P(1)	116.8(2)		

Table 8 Atomic coordinates ($\times 10^4$) for $[Ru_4H(CO)_{10}(dppe)BH_2]\cdot CH_2Cl_2$

Atom	*x*	*y*	*z*	Atom	*x*	*y*	*z*
Ru(1)	3 332(1)	6 728(1)	154(1)	C(10)	3 158(8)	7 159(6)	−1 927(5)
Ru(2)	1 519(1)	5 990(1)	−74(1)	C(11)	3 804(5)	8 949(5)	529(4)
Ru(3)	1 787(1)	7 495(1)	776(1)	C(12)	3 601(5)	8 848(5)	1 319(4)
Ru(4)	2 349(1)	6 662(1)	−1 260(1)	C(21)	5 927(6)	8 658(7)	546(5)
B	2 067(6)	7 305(5)	−297(4)	C(22)	6 834(7)	8 613(8)	825(6)
P(1)	4 212(1)	7 976(1)	98(1)	C(23)	7 220(6)	7 877(9)	1 054(6)
P(2)	2 362(1)	8 727(1)	1 346(1)	C(24)	6 733(7)	7 170(9)	1 000(7)
Cl(1)	9 734(4)	1 256(4)	1 533(3)	C(25)	5 806(6)	7 163(7)	728(6)
Cl(2)	8 790(3)	−270(4)	1 891(2)	C(26)	5 394(5)	7 905(6)	500(4)
O(1)	4 699(6)	5 630(5)	−570(5)	C(31)	3 797(8)	9 007(6)	−1 128(5)
O(2)	4 102(4)	6 377(5)	1 700(4)	C(32)	3 975(11)	9 360(8)	−1 792(6)
O(3)	813(5)	5 302(4)	1 305(4)	C(33)	4 721(12)	9 121(10)	−2 114(6)
O(4)	−326(5)	6 635(4)	−685(4)	C(34)	5 307(8)	8 529(10)	−1 789(5)
O(5)	1 380(5)	4 210(4)	−779(5)	C(35)	5 148(7)	8 161(8)	−1 140(5)
O(6)	−178(4)	7 770(4)	1 066(4)	C(36)	4 408(5)	8 417(5)	−793(4)
O(7)	2 199(4)	6 557(4)	2 192(3)	C(41)	2 247(6)	10 515(5)	1 329(5)
O(8)	672(7)	6 444(7)	−2 322(5)	C(42)	2 007(8)	11 314(6)	1 046(6)
O(9)	3 073(8)	4 882(5)	−1 555(5)	C(43)	1 436(7)	11 373(6)	435(5)
O(10)	3 596(6)	7 396(5)	−2 348(4)	C(44)	1 116(6)	10 639(5)	80(5)
C(1)	4 178(7)	6 057(6)	−299(6)	C(45)	1 398(5)	9 836(5)	363(4)
C(2)	3 790(5)	6 511(5)	1 117(5)	C(46)	1 948(5)	9 765(4)	984(4)
C(3)	1 103(6)	5 588(5)	806(5)	C(51)	1 277(6)	9 004(8)	2 452(4)
C(4)	362(6)	6 377(5)	−460(5)	C(52)	1 050(7)	9 046(8)	3 145(5)
C(5)	1 455(7)	4 877(5)	−527(5)	C(53)	1 698(7)	8 901(7)	3 713(5)
C(6)	562(5)	7 700(5)	961(4)	C(54)	2 565(6)	8 708(6)	3 564(4)
C(7)	2 061(5)	6 895(5)	1 651(4)	C(55)	2 807(6)	8 664(5)	2 860(4)
C(8)	1 312(9)	6 510(7)	−1 940(5)	C(56)	2 150(5)	8 806(5)	2 292(4)
C(9)	2 783(10)	5 531(7)	−1 432(7)	C(100)	9 106(11)	913(12)	2 102(8)

Table 9 Selected bond distances (Å) and angles (°) for *trans*-$[Ru_4H(CO)_{10}(dppe)BH_2]\cdot CH_2Cl_2$

Ru(1)–Ru(2)	2.901(1)	Ru(1)–Ru(3)	2.897(1)
Ru(2)–Ru(3)	2.828(1)	Ru(1)–Ru(4)	2.891(1)
Ru(2)–Ru(4)	2.816(1)	Ru(1)–B	2.168(8)
Ru(2)–B	2.246(8)	Ru(3)–B	2.095(8)
Ru(4)–B	2.124(8)	Ru(3)–P(2)	2.310(2)
Ru(1)–P(1)	2.337(2)		
Ru(2)–Ru(1)–Ru(3)	58.4(1)	Ru(2)–Ru(1)–Ru(4)	58.2(1)
Ru(3)–Ru(1)–Ru(4)	91.8(1)	Ru(1)–Ru(2)–Ru(3)	60.7(1)
Ru(1)–Ru(2)–Ru(4)	60.7(1)	Ru(3)–Ru(2)–Ru(4)	94.8(1)
Ru(1)–Ru(3)–Ru(2)	60.9(1)	Ru(1)–Ru(4)–Ru(2)	61.1(1)
Ru(2)–Ru(3)–P(2)	165.3(1)	Ru(1)–Ru(3)–P(2)	104.8(1)
Ru(3)–Ru(1)–P(1)	97.8(1)	Ru(2)–Ru(1)–P(1)	145.8(1)
Ru(4)–Ru(1)–P(1)	102.9(1)	Ru(4)–Ru(2)–B	48.0(2)
Ru(2)–Ru(1)–B	50.1(2)	Ru(3)–Ru(1)–B	46.2(2)
Ru(1)–Ru(2)–B	47.8(2)	Ru(3)–Ru(2)–B	47.1(2)
Ru(1)–Ru(3)–B	48.3(2)	Ru(2)–Ru(3)–B	51.7(2)
Ru(2)–Ru(4)–B	51.8(2)	Ru(4)–Ru(1)–B	47.0(2)
Ru(1)–Ru(4)–B	48.3(2)	Ru(3)–B–Ru(4)	160.0(4)
Ru(1)–B–Ru(2)	82.1(3)	B–Ru(1)–P(1)	95.8(2)
B–Ru(3)–P(2)	117.3(2)		

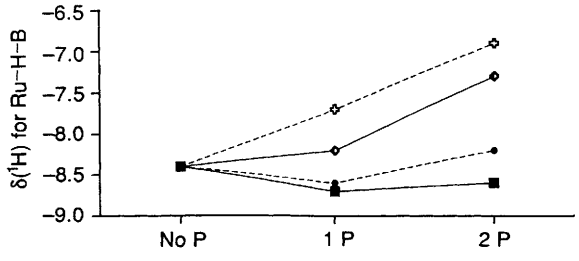

Fig. 6 Effect of phosphine substitution of the chemical shifts of the Ru–H–B protons in the ^1H NMR spectra of $[Ru_4H(CO)_{11}(dppp)BH_2]$ (pendant, Fig. 4), $[Ru_4H(CO)_{10}(dppp)BH_2]$ (chelate, Fig. 4), $[Ru_4H(CO)_{11}(dppf)BH_2]$ (pendant, Fig. 4) and $[Ru_4H(CO)_{11}(dppp)BH_2]$ (chelate, Fig. 4): ◆, dppp, H remote from P; ■, dppp, H adjacent to P; ✿, dppf, H remote from P; ●, dppf, H adjacent to P

≈20% yield. These were spectroscopically characterised (Tables 1 and 2), and similarities between the data for the dppp, dppb and dpph analogues assist in the structural assignments. Attempts to crystallise $[Ru_4H(CO)_{11}(dppf)BH_2]$ from CH_2Cl_2 solution led instead to the formation of $[\{Ru_4H(CO)_{11}BH_2\}_2(\mu\text{-dppf})]$. Repeating the reaction under conditions of photolysis and a two-fold excess of ligand (method II) yielded, in addition to unreacted starting cluster, $[Ru_4H(CO)_{11}(dppf)BH_2]$ (≈10%), $[\{Ru_4H(CO)_{11}BH_2\}_2(\mu\text{-dppf})]$ (≈15%) and the yellow-orange compound $[Ru_4H(CO)_{10}(dppf)BH_2]$ (≈15%). A comparison of the data for this last compound with those for the dppp analogue, and application of the same arguments (see above), allow us to propose the formation of a product with the dppf ligand chelating to one wing-tip ruthenium atom. The shifts of the signals for the Ru–H–B protons in the ^1H NMR spectra of the products (Fig. 6) exhibit similar trends to those described earlier for the dppp derivatives.

Reaction with dppa. The bis(diphenylphosphino)acetylene ligand possesses a rigid carbon backbone and therefore its modes of co-ordination to a metal centre or multimetal framework are more restricted than those of diphosphines discussed so far. This ligand has been used successfully to link transition-metal clusters.[26] Chromatographic separation of the products of the reaction of equimolar amounts of dppa and $[Ru_4H(CO)_{12}BH_2]$ in CH_2Cl_2 at room temperature for 8 d yielded three fractions although significant material remained on the baseline and was not extracted. The first (yellow) band comprised $[Ru_4H_4(CO)_{12}]$[1] whilst the other products were identified as yellow-orange $[Ru_4H(CO)_{11}(dppa)BH_2]$ (≈15%) and yellow $[\{Ru_4H(CO)_{11}BH_2\}_2(\mu\text{-dppa})]$ (≈40%).

The similarity between the carbonyl regions of the infrared spectra of the two substituted products and their resemblance to those of other monosubstituted clusters in this study initially suggested identities for the products as $[Ru_4H(CO)_{11}(dppa)BH_2]$ and $[\{Ru_4H(CO)_{11}BH_2\}_2(\mu\text{-dppa})]$. This result was supported by mass spectrometric and NMR spectroscopic data (Table 1). Thus, substitution of one P-donor atom occurs at a wing-tip ruthenium site as in all previous examples of this family of clusters. When the reaction conditions were altered to those of method II (photolysis and four-fold excess of ligand) $[Ru_4H(CO)_{11}(dppa)BH_2]$ was formed in (typically) 30% yield but was not accompanied by the production of the linked species. The second product in this reaction proved to be the disubstituted cluster $[Ru_4H(CO)_{10}(dppa)_2BH_2]$.

A single ^{11}B NMR resonance is observed for $[Ru_4H(CO)_{10}(dppa)_2BH_2]$ and the shift is similar to those of $[Ru_4H(CO)_{11}(dppa)BH_2]$ and $[\{Ru_4H(CO)_{11}BH_2\}_2(\mu\text{-dppa})]$ (Table 1). The ^1H NMR spectrum of $[Ru_4H(CO)_{10}(dppa)_2BH_2]$ shows, in addition to signals for the phenyl protons, a broad resonance at δ −6.5 (Ru–H–B) and a sharper signal at δ −20.7 for which coupling to the ^{31}P nuclei could not be resolved. The ^{31}P NMR spectrum exhibits two resonances (δ +11.3 and +9.0) with relative integrals 5:4, in addition to a higher-field signal at δ −33.0 (relative integral 9). This latter shift compares favourably with that observed for free dppa (δ −32), and thus these data indicate the presence of two isomers of $[Ru_4H(CO)_{10}(dppa)_2BH_2]$, each containing pendant dppa ligands. The IR spectrum of $[Ru_4H(CO)_{10}(dppa)_2BH_2]$ is quite similar to those of disubstituted derivatives of the type $[Ru_4H(CO)_{10}(PR_3)_2BH_2]$ (Table 2) and we propose the structures shown in Fig. 7 for the isomers of $[Ru_4H(CO)_{10}(dppa)_2BH_2]$. We were unable to observe a parent ion in the mass spectrum of $[Ru_4H(CO)_{10}(dppa)_2BH_2]$; the highest-mass envelope was centred around *m/z* 1090 and this mass and the isotopic distribution are consistent with a fragment formulation of $\{Ru_4H(CO)_{10}(dppa)BH_2\}$. This in itself is not evidence for the formation of the disubstituted product since the same fragment could arise from the loss of CO from $[Ru_4H(CO)_{11}(dppa)BH_2]$. However, the mass spectrum of $[Ru_4H(CO)_{11}(dppa)BH_2]$ *repeatedly* produces the highest-mass envelope which is assigned to the parent ion plus an oxygen atom as we have noted for other clusters with pendant diphosphine ligands.

Conclusion

The tertiary phosphines PPh_3 and $P(C_6H_{11})_3$ react with $[Ru_4H(CO)_{12}BH_2]$ with the first carbonyl substitution occurring in the wing-tip equatorial site (*e.g.* site 4, Fig. 1). The second substitution gives rise to either a [4,10] or [4,12] pattern in the case of PPh_3, but for $P(C_6H_{11})_3$ a [4,10] pattern is preferred due to the steric demands of the ligand. With a 30-fold excess of the less sterically demanding phosphite $P(OMe)_3$, the reaction gives the di-, tri- and tetra-substituted products with substitution patterns of [4,10] or [4,12] for the two isomers of $[Ru_4H(CO)_{10}\{P(OMe)_3\}_2BH_2]$, and of [4,7,10] and [1,4,7,10] for $[Ru_4H(CO)_9\{P(OMe)_3\}_3BH_2]$ and $[Ru_4H(CO)_8\{P(OMe)_3\}_4BH_2]$ respectively. This gives the sterically favoured 'paddle-wheel' arrangement of $P(OMe)_3$ ligands.

With diphosphine ligands there is the possibility of chelation, edge-bridging or pendant modes within a single cluster, or the linkage of two clusters *via* a diphosphine molecule. The dppe ligand favours an edge-bridging mode with the formation of two isomers exhibiting [2,4] or [3,4] substitution patterns (Fig. 1) but there is some competition for the formation of the linked species $[\{Ru_4H(CO)_{11}BH_2\}_2(\mu\text{-dppe})]$. Increasing the carbon backbone by one methylene unit has the effect of swinging the reaction pathway in favour of products in which the diphosphine ligand is pendant or chelating (Fig. 4). The

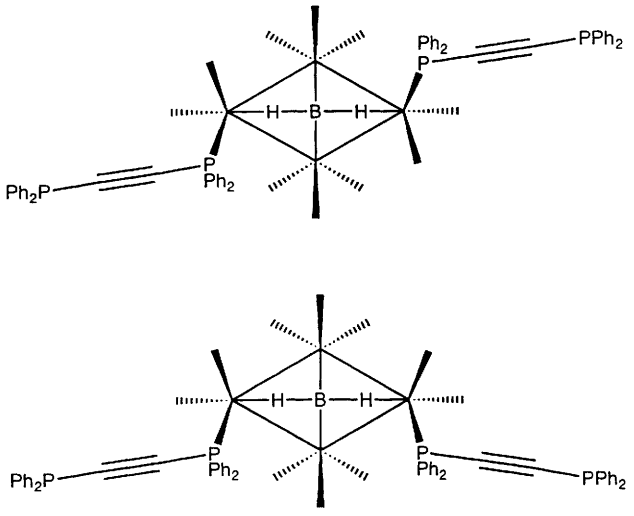

Fig. 7 Proposed isomers of $[Ru_4H(CO)_{10}(dppa)_2BH_2]$

formation of the linked species was only observed under non-photolytic conditions, and this appeared to be at the expense of chelation of the dppp ligand to a single wing-tip ruthenium centre. A similar scenario was observed for the dppf ligand. Longer methylene backbones (dppb and dpph, L–L) favoured the formation of product types $[Ru_4H(CO)_{11}(L–L)BH_2]$ and $[\{Ru_4H(CO)_{11}BH_2\}_2(\mu\text{-}L–L)]$. With its rigid acetylenic backbone, dppa reacts with $[Ru_4H(CO)_{12}BH_2]$ to give a distribution of products similar to those of the longer-chain bis(diphenylphosphino)alkane ligands, but additionally when the dppa is in a four-fold excess disubstitution occurs to yield isomers of $[Ru_4H(CO)_{10}(dppa)_2BH_2]$ with [4,10]- or [4,12]-substitution patterns (Fig. 7). The dppa-substituted clusters in particular provide the opportunity for the controlled linkage of cluster–mononuclear metal or cluster–cluster fragments, and preliminary studies have already shown that $[Ru_4H(CO)_{11}(dppa)BH_2]$ reacts with $[W(CO)_5(NCMe)]$ to give $[Ru_4H(CO)_{11}BH_2(\mu\text{-}dppa)W(CO)_5]$ or with $[Os_3(CO)_{11}(NCMe)]$ to give $[Ru_4H(CO)_{11}BH_2(\mu\text{-}dppa)Os_3(CO)_{11}]$.[27]

We have not yet carried out a systematic study of the reaction between $[Ru_4H(CO)_{12}BH_2]$ and a particular phosphine to investigate how the product distribution varies with a change in the cluster : ligand ratio.

Acknowledgements

We thank the donors of the Petroleum Research Fund, administered by the American Chemical Society, for support of this work (grant no. 25533-AC3), the SERC for studentships (to S. M. D. and J. S. H.) and the National Science Foundation for a grant (CHE 9007852) towards the purchase of a diffractometer at the University of Delaware.

References

1 C. R. Eady, B. F. G. Johnson and J. Lewis, *J. Chem. Soc., Dalton Trans.*, 1977, 477.
2 F.-E. Hong, D. A. McCarthy, J. P. White III, C. E. Cottrell and S. G. Shore, *Inorg. Chem.*, 1990, **29**, 2874.
3 A. K. Chipperfield, C. E. Housecroft and A. L. Rheingold, *Organometallics*, 1990, **9**, 681.
4 C. E. Housecroft, *Coord. Chem. Rev.*, 1995, in the press and refs. therein.
5 C. E. Housecroft, *Chem. Soc. Rev.*, 1995, **24**, 215 and refs. therein.
6 C. E. Housecroft, J. S. Humphrey, A. K. Keep, D. M. Matthews, N. J. Seed, B. S. Haggerty and A. L. Rheingold, *Organometallics*, 1992, **11**, 4048.
7 C. E. Housecroft and T. P. Fehlner, *Organometallics*, 1986, **5**, 1279; C. E. Housecroft, M. L. Buhl, G. J. Long and T. P. Fehlner, *J. Am. Chem. Soc.*, 1987, **109**, 3323.
8 D. Braga, B. F. G. Johnson, J. Lewis, J. M. Mace, M. McPartlin, J. Puga, W. J. H. Nelson and P. R. Raithby, *J. Chem. Soc., Chem. Commun.*, 1982, 1081.
9 A. Gourdin and Y. Jeannin, *J. Organomet. Chem.*, 1992, **440**, 353.
10 J. R. Galsworthy, C. E. Housecroft, D. M. Matthews, R. Ostrander and A. L. Rheingold, *J. Chem. Soc., Dalton Trans.*, 1994, 69.
11 M. L. Blohm, D. E. Fjare and W. L. Gladfelter, *J. Am. Chem. Soc.*, 1986, **108**, 2301.
12 U. Casellato, D. Ajo, G. Valle, B. Corain, B. Longato and R. Graziani, *J. Crystallogr. Spectrosc.*, 1988, **18**, 583.
13 S. Onaka, A. Mizuno and S. Takagi, *Chem. Lett.*, 1989, 2037.
14 D. T. Hill, G. R. Girard, F. L. McCabe, R. K. Johnson, P. D. Stupik, J. H. Zhang, W. M. Reiff and D. S. Eggleston, *Inorg. Chem.*, 1989, **28**, 3529.
15 A. Houlton, D. M. P. Mingos, D. M. Murphy, D. J. Williams, L.-T. Phang and T. S. A. Hor, *J. Chem. Soc., Dalton Trans.*, 1993, 3629.
16 L.-T. Phang, S. C. F. Yeung, T. S. A. Hor, S. B. Khoo, Z.-Y. Zhou and T. C. W. Mak, *J. Chem. Soc., Dalton Trans.*, 1993, 165.
17 J. T. Lin, S. Y. Wang, P. S. Huang, Y. M. Hsiao, Y. S. Wen and S. K. Yeh, *J. Organomet. Chem.*, 1990, **388**, 151.
18 See, for example, M. I. Bruce, I. R. Butler, W. R. Cullen, G. A. Koutsantonis, M. R. Snow and E. R. T. Tiekink, *Aust. J. Chem.*, 1988, **41**, 963; T. M. Miller, K. J. Ahmed and M. S. Wrighton, *Inorg. Chem.*, 1989, **28**, 2347; A. L. Rheingold, B. S. Haggerty, A. J. Edwards, C. E. Housecroft, A. D. Hattersley and N. Hinze, *Acta Crystallogr., Sect. C*, 1994, **50**, 1411; B. S. Haggerty, C. E. Housecroft, A. L. Rheingold and B. A. M. Shaykh, *J. Chem. Soc., Dalton Trans.*, 1991, 2175 and refs. therein.
19 G. M. Sheldrick, SHELXTL-PC software versions 4 or 5, Siemens XRD, Madison, WI.
20 S. M. Draper, Ph.D. Thesis, University of Cambridge, 1991.
21 C. A. Tolman, *Chem. Rev.*, 1977, **77**, 313.
22 See, for example, M. I. Bruce, M. J. Liddell, O. bin Shawkataly, I. Bytheway, B. W. Skelton and A. H. White, *J. Organomet. Chem.*, 1988, **347**, 207; M. I. Bruce, J. G. Matisons and B. K. Nicholson, *J. Organomet. Chem.*, 1983, **247**, 321; S. A. R. Knox and H. D. Kaesz, *J. Am. Chem. Soc.*, 1971, **93**, 4594.
23 C. E. Housecroft, B. A. M. Shaykh, A. L. Rheingold and B. S. Haggerty, *Inorg. Chem.*, 1991, **30**, 125.
24 See, for example, Y. K. Yan, H. S. O. Chan, T. S. A. Hor, K.-L. Tan, L.-K. Liu and Y.-S. Wen, *J. Chem. Soc., Dalton Trans.*, 1992, 423.
25 See, for example, (*a*) S. T. Chacon, W. R. Cullen, M. I. Bruce, O. bin Shawkataly, F. W. B. Einstein, R. H. Jones and A. C. Willis, *Can. J. Chem.*, 1990, **68**, 2001; (*b*) S. Onaka, A. Mizuno and S. Takagi, *Chem. Lett.*, 1989, 2037; (*c*) T.-J. Kim, S.-C. Kwon, Y.-H. Kim, N. H. Heo, M. M. Teeter and A. Yamano, *J. Organomet. Chem.*, 1991, **426**, 71.
26 See, for example, O. Orama, *J. Organomet. Chem.*, 1986, **314**, 273; E. Sappa, *J. Organomet. Chem.*, 1988, **352**, 327; M. I. Bruce, M. L. Williams, J. M. Patrick and A. H. White, *J. Chem. Soc., Dalton Trans.*, 1985, 1229; M. I. Bruce, M. J. Liddell and E. R. T. Tiekink, *J. Organomet. Chem.*, 1990, **391**, 81; A. J. Amoroso, B. F. G. Johnson, J. Lewis, A. D. Massey, P. R. Raithby and W.-T. Wong, *J. Organomet. Chem.*, 1992, **440**, 219.
27 J. S. Humphrey, Ph.D. Thesis, University of Cambridge, 1995.

Received 14*th June* 1995; *Paper* 5/03856A